Quasi-continental Sentinel-1 InSAR Investigation of Land Subsidence and Aquifer-system Storage Loss in Central Mexico

Francesca Cigna[1], Deodato Tapete[2]

[1] National Research Council (CNR-ISAC), Italy
[2] Italian Space Agency (ASI)

National Research Council

Agenzia Spaziale Italiana

FRINGE 2023

University of Leeds, UK | 11 - 15 September 2023

Groundwater exploitation and aquifer depletion in Mexico

Aquifers provide 40% of the consumed water of Mexico, i.e. **~35,300 hm³/year**, which is used for agriculture (71%), public supply (21%), industry (8%)

DMA (Annual GW Availability) = *recharge – natural discharge – licensed pumping*

Overexploited if *pumping/recharge* ≥ 1.1

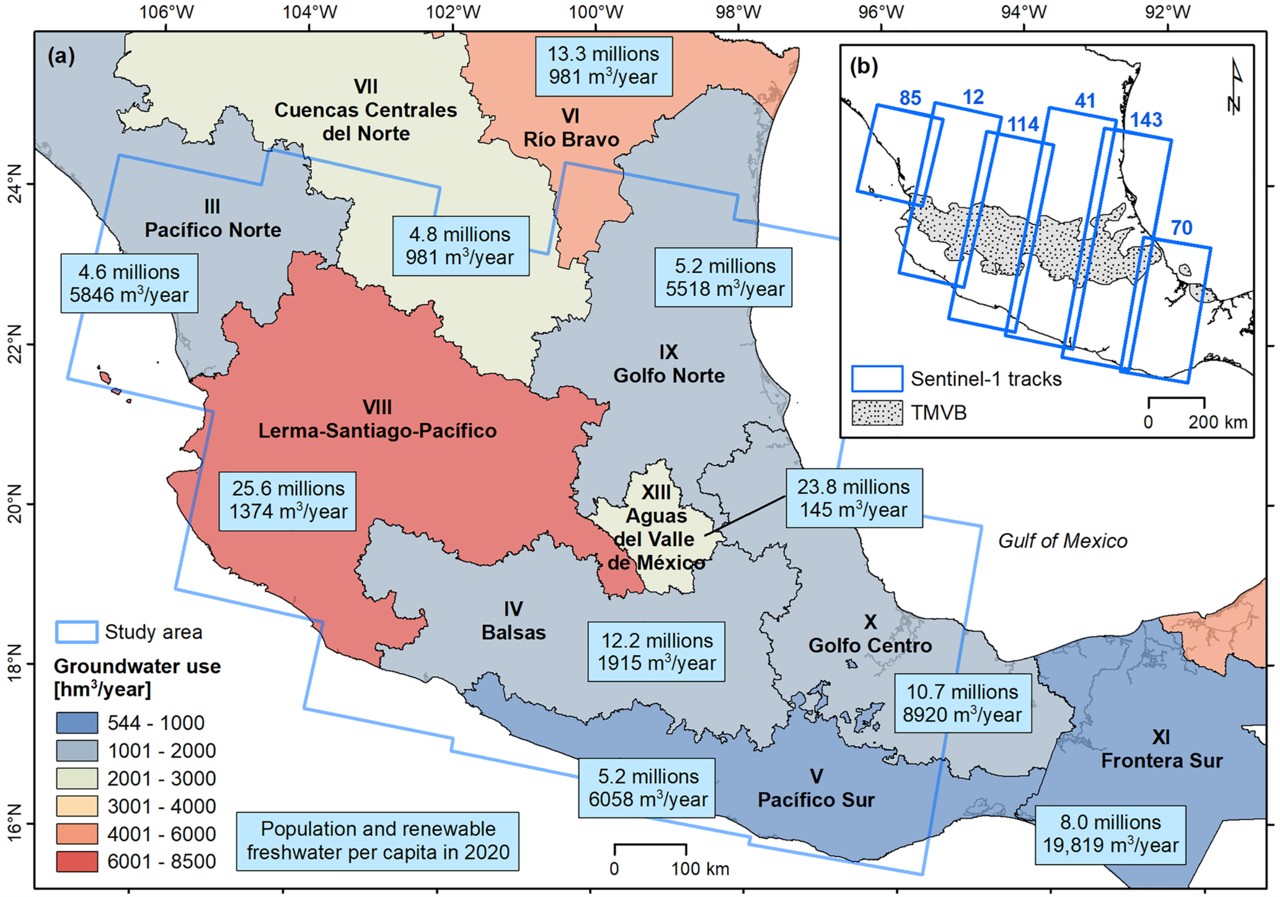

CIGNA & TAPETE, *2022, doi: 10.1029/2022GL098923*

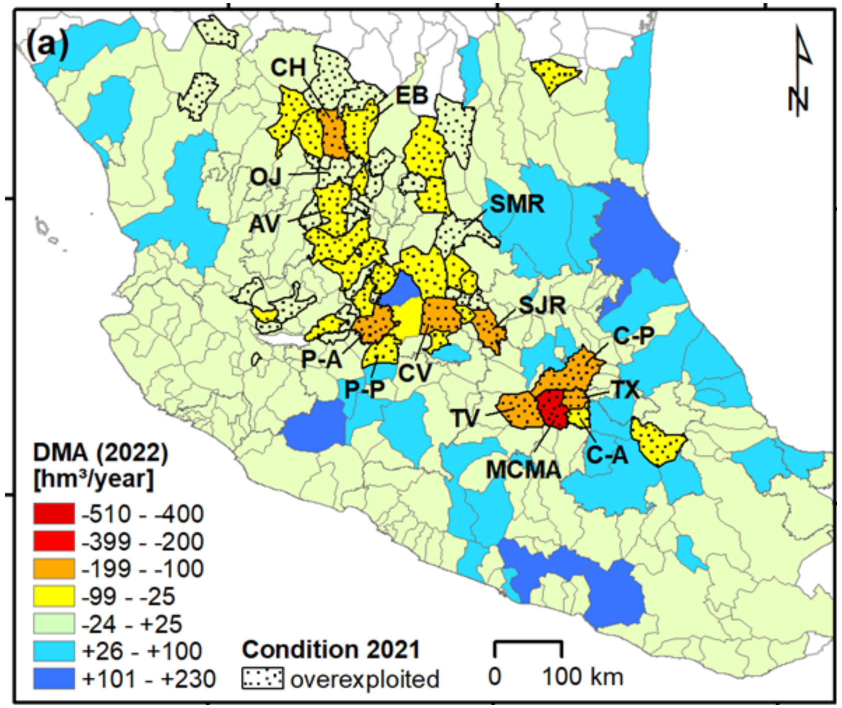

Mexico is not a "*water-poor*" country, though shows large spatial and temporal discrepancies in recharge/consumption rates

As of 2022, >**200 aquifers in deficit and** >**100 overexploited**, of which 57 in Central Mexico (>85.2 M inhab., ~68% tot pop.)

Groundwater exploitation and aquifer depletion in Mexico

Aquifer-system storage change (*ΔS*)

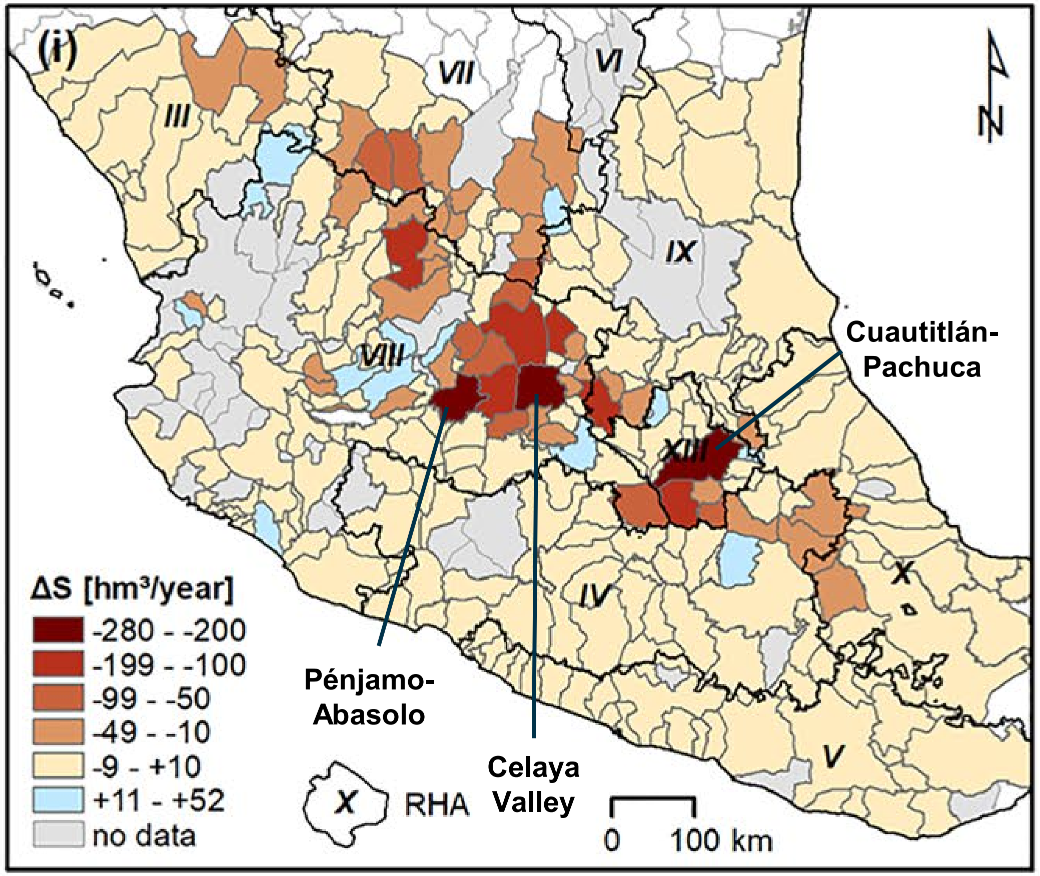

CIGNA & TAPETE, *2022, doi: 10.1029/2022GL098923*

Groundwater management reports by CONAGUA (*National Water Commission*), show that **a number of aquifer-systems are losing part of their storage capacity and compacting**

ΔS is the volumetric difference between recharge (R) and natural and human-induced discharge (D) in a given time period, and depends on hydraulic head change (*Δh*) and storage coefficient or storativity (S) and surface (A) of the aquifer-system

$$\Delta S = R - D = S * A * \Delta h$$

Highly exploited aquifer-systems loosing non-renewable storage are concentrated in the central sector of the region

***ΔS* loss rate reaches**

−280 hm^3/year (Cuautitlán-Pachuca)
−215 hm^3/year (Pénjamo-Abasolo)
−201 hm^3/year (Celaya Valley)

resulting from groundwater withdrawal of 637, 440 and 515 hm^3/year, respectively

Land subsidence and impacts in urban environments

Land subsidence resulting from groundwater overexploitation has been documented in major cities

Severe **impacts on infrastructure** such as public/private buildings, roads and utility networks:
e.g. cracks, surface faults, tilted buildings, seeming uplift of deeply-founded structures

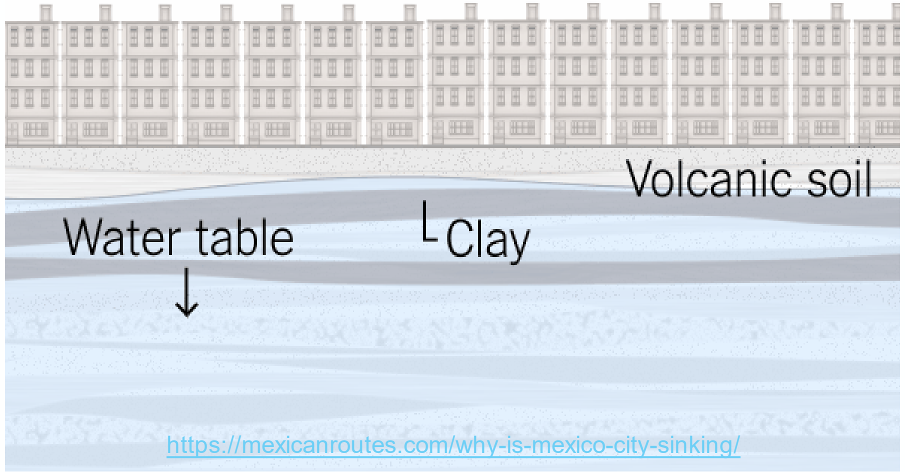

Unlevel sinking and undulating rooflines in Mexico City (www.sciencemag.org)

Fissuring and cracking of houses due to differential subsidence (FIGUEROA-MIRANDA *et al.* 2018)

Fissured and ramped urban roads and ground due to **surface faulting** in Aguascalientes (©INEGI 2020)

Quasi-continental Sentinel-1 InSAR survey

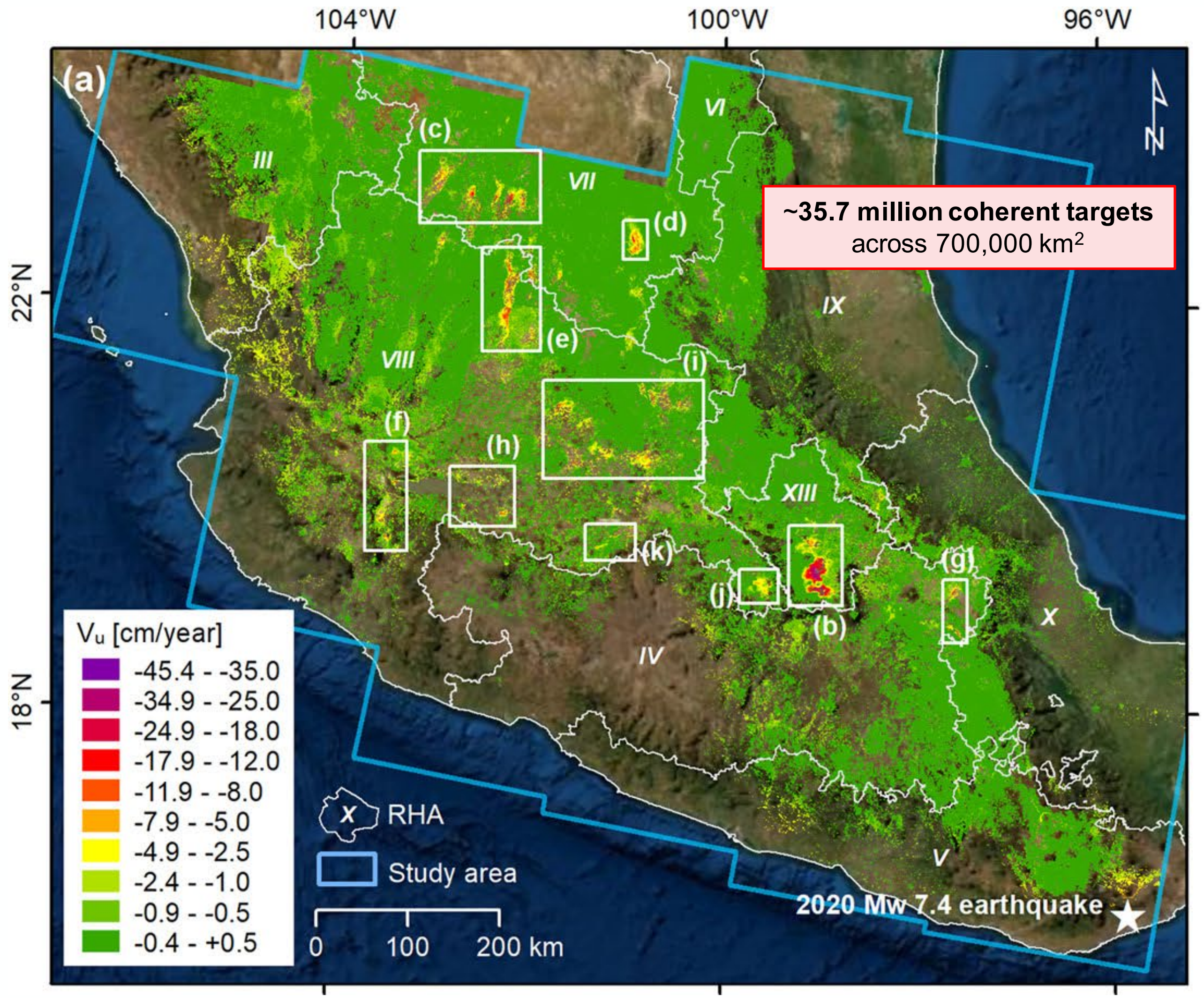

CIGNA & TAPETE, *2022, doi: 10.1029/2022GL098923*

Input: **~1700 Sentinel-1 IW scenes**, 2 year-long period (2019-2020)

Method: **Parallel-SBAS** workflow

Infrastructure: geohazards tep

ESA NoR project id.190791

Results: **30+ subsidence "*hotspots*"**

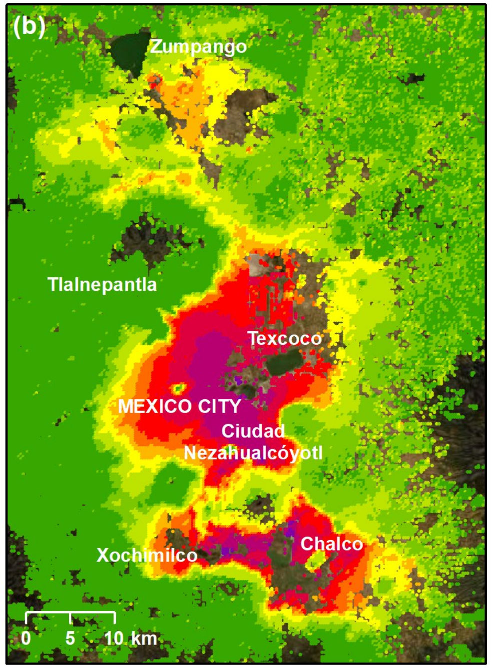

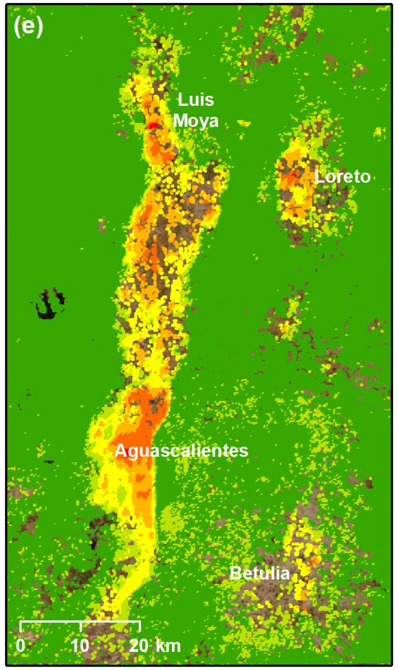

Correlation between land subsidence and aquifer-system balance parameters in Central Mexico

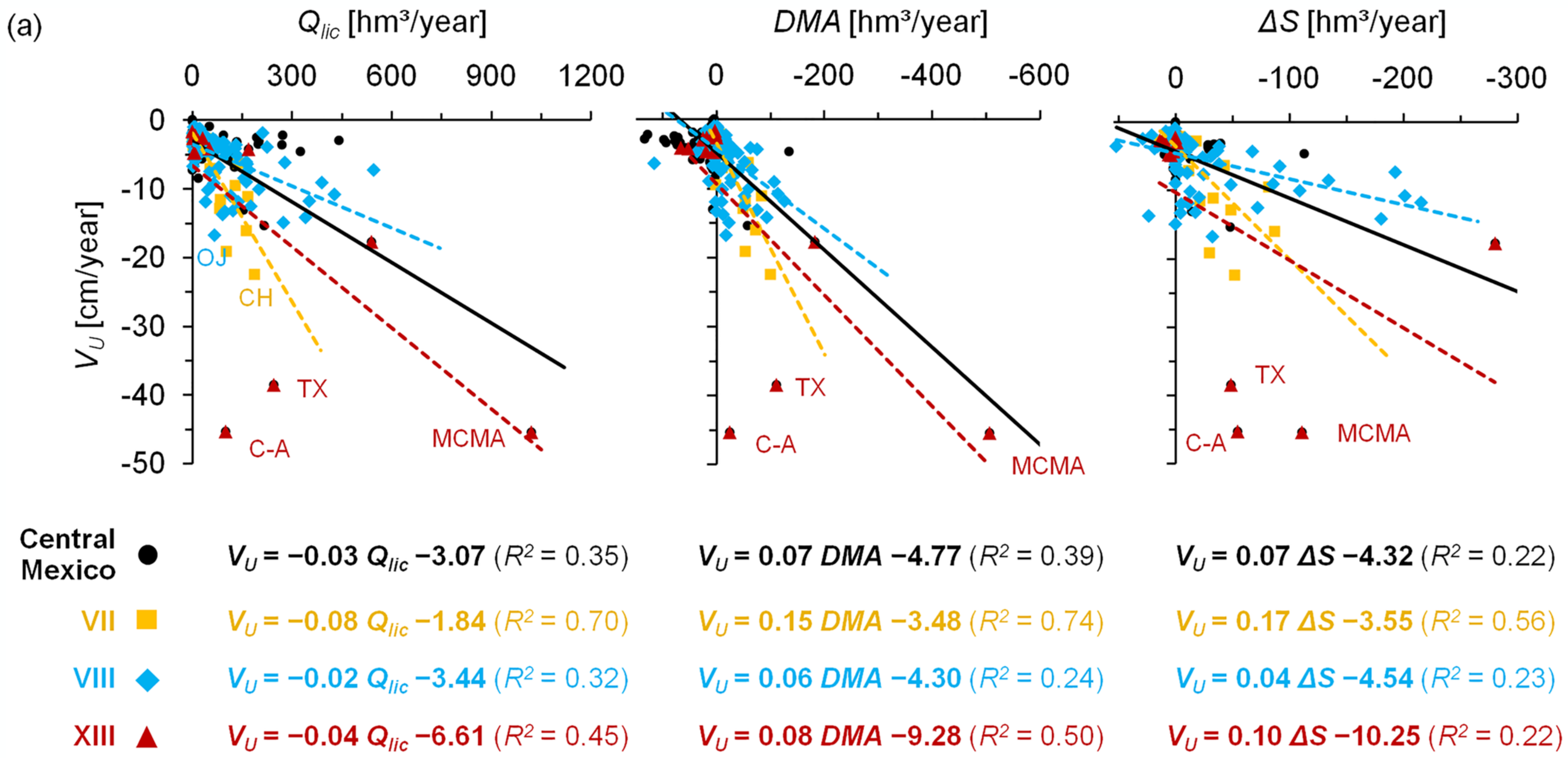

CIGNA & TAPETE, *2022, doi: 10.1029/2022GL098923*

- InSAR-derived VU fairly correlates with aquifer-system balance parameters.
- Approximately 40% of the observed VU variation across Central Mexico is explained by DMA variance. The figure drops to 35% and 22% when considering total extraction volume (Qlic) and Aquifer-system storage change (ΔS), respectively.
- The three hydrological-administrative regions incl. most hotspots generally show higher correlation with each parameter.

Correlation between land subsidence and aquifer-system balance parameters in Central Mexico. Licensed groundwater withdrawal (Qlic), annual groundwater availability (DMA) and modeled storage change (ΔS) are compared with Interferometric Synthetic Aperture Radar (InSAR)-derived (a) highest (negative) vertical displacement velocity (VU).

Notation: AV, Aguascalientes Valley; C-A, Chalco-Amecameca; CH, Chupaderos; MCMA, Mexico City Metropolitan Area; OJ, Ojocaliente; TX, Texcoco.

Correlation between land subsidence and aquifer-system balance parameters in Central Mexico

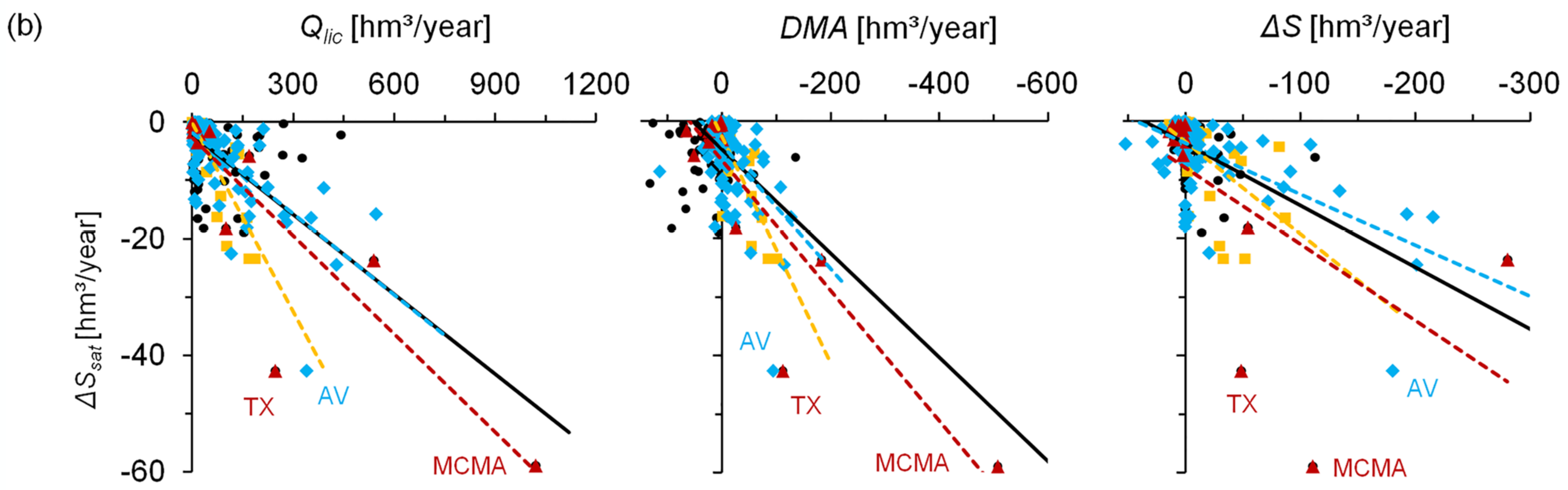

	ΔS_{sat} vs Q_{lic}	ΔS_{sat} vs DMA	ΔS_{sat} vs ΔS
Central Mexico ●	$\Delta S_{sat} = -0.05\ Q_{lic} - 2.09$ ($R^2 = 0.47$)	$\Delta S_{sat} = 0.09\ DMA - 4.77$ ($R^2 = 0.35$)	$\Delta S_{sat} = 0.11\ \Delta S - 3.88$ ($R^2 = 0.31$)
VII ■	$\Delta S_{sat} = -0.11\ Q_{lic} - 0.36$ ($R^2 = 0.68$)	$\Delta S_{sat} = 0.19\ DMA - 2.65$ ($R^2 = 0.67$)	$\Delta S_{sat} = 0.16\ \Delta S - 3.57$ ($R^2 = 0.28$)
VIII ◆	$\Delta S_{sat} = -0.05\ Q_{lic} - 1.78$ ($R^2 = 0.50$)	$\Delta S_{sat} = 0.10\ DMA - 4.02$ ($R^2 = 0.24$)	$\Delta S_{sat} = 0.09\ \Delta S - 3.79$ ($R^2 = 0.37$)
XIII ▲	$\Delta S_{sat} = -0.06\ Q_{lic} - 2.75$ ($R^2 = 0.78$)	$\Delta S_{sat} = 0.11\ DMA - 6.72$ ($R^2 = 0.81$)	$\Delta S_{sat} = 0.13\ \Delta S - 7.97$ ($R^2 = 0.33$)

CIGNA & TAPETE, *2022, doi: 10.1029/2022GL098923*

Correlations improve for the InSAR-derived aquifer-system compaction ΔSsat, which appears much better explained by Qlic (47%) and ΔS (30%) across the whole area.

Single aquifer-systems often compact more than others within the RHA, for example, −0.18 ΔSsat/Qlic rate is observed at Chalco-Amecameca and Texcoco, three-times steeper than region XIII's. Similarly, at Ojocaliente ΔSsat/Qlic is −0.12, two-times steeper than region VIII's.

Correlation between land subsidence and aquifer-system balance parameters in Central Mexico. Licensed groundwater withdrawal (Qlic), annual groundwater availability (DMA) and modeled storage change (ΔS) are compared with Interferometric Synthetic Aperture Radar (InSAR)-derived (b) total compaction volume rate (ΔSsat) at each aquifer-system.

Notation: AV, Aguascalientes Valley; C-A, Chalco-Amecameca; CH, Chupaderos; MCMA, Mexico City Metropolitan Area; OJ, Ojocaliente; TX, Texcoco

Accuracy of InSAR-derived displacement velocity vs. geodetic data

Displacement velocities from InSAR and GNSS

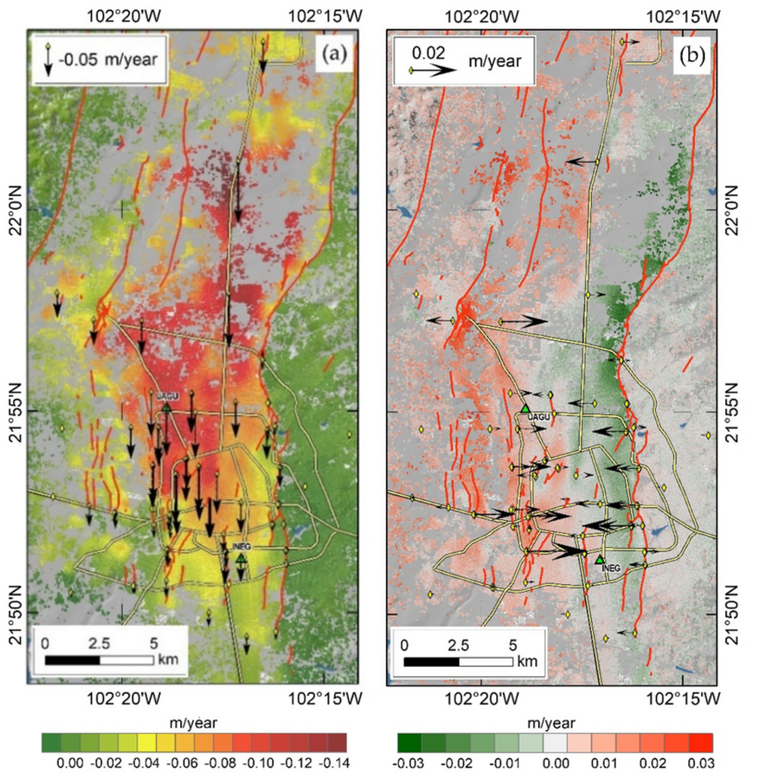

Vertical velocity, V_U E-W velocity, V_E

PSI-SBAS inter-comparison

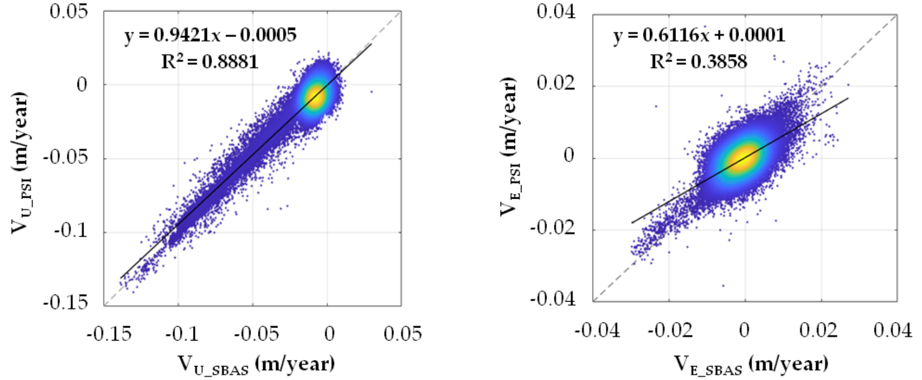

Accuracy assessment against GNSS and leveling

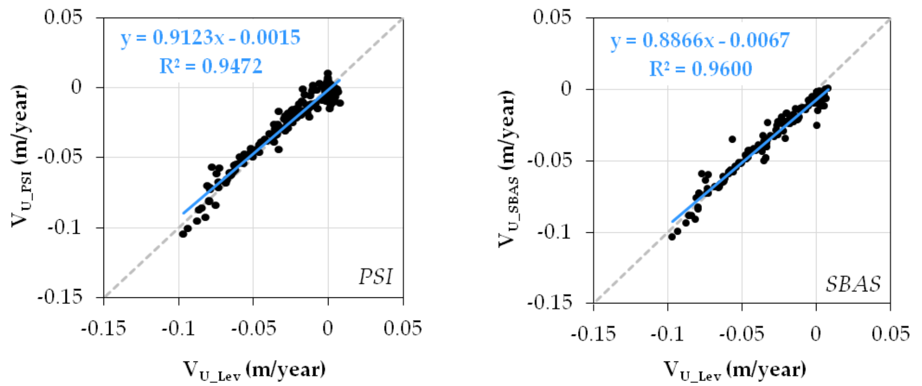

Geodetic data by INEGI: *National Institute of Statistics, Geography and Informatics*

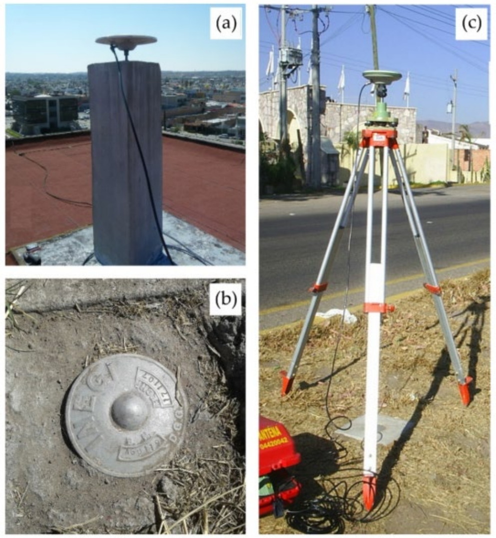

- Accuracy was estimated against permanent GNSS, static GNSS benchmark repositioning and geodetic leveling monitoring data
- V_U **differences of 8–10 mm/year** (standard deviations) and **relative errors < 20%** for locations subsiding faster than −15 mm/year

CIGNA *et al.* 2021, doi:10.3390/rs13234800

Hotspot #1 Mexico City: Vertical velocity field vs. geology

V_U in 2017–2019

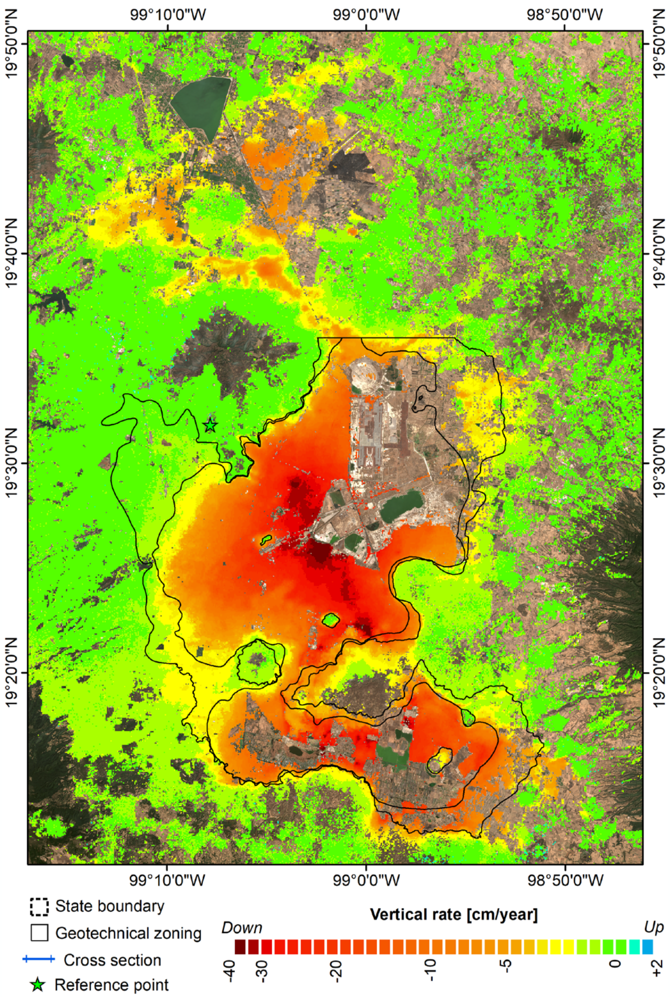

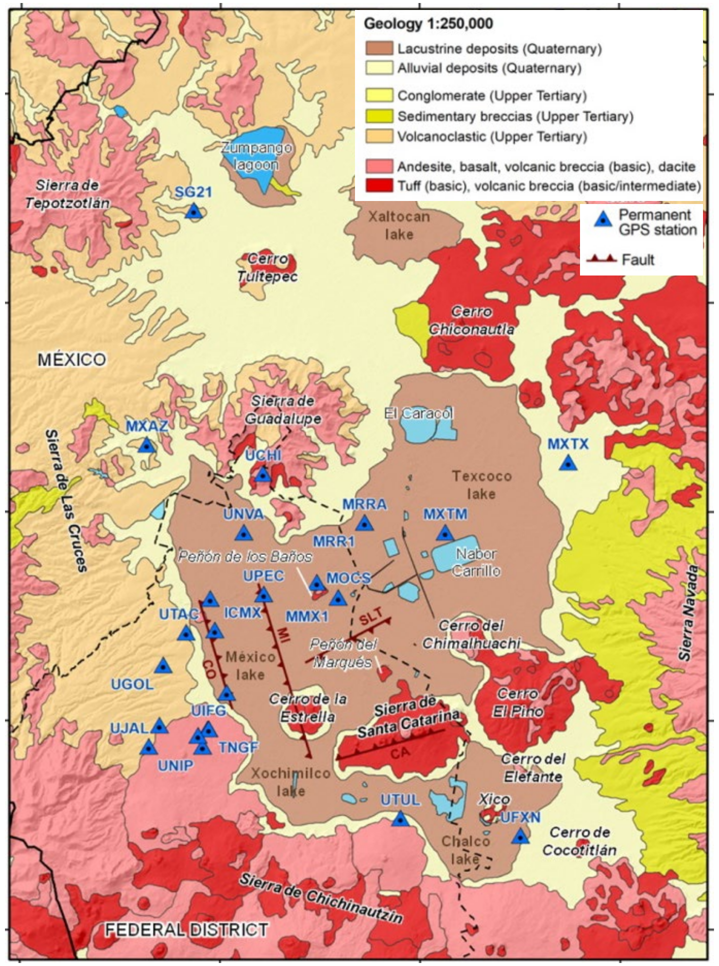

CIGNA & TAPETE 2021, doi:10.1016/j.rse.2020.112161

→ **Highest rates at the lacustrine deposits** (compressible clay and silt-rich deposits composing the aquitard)

→ Stability at hard volcanic rocks

H_C aquitard thickness [m]

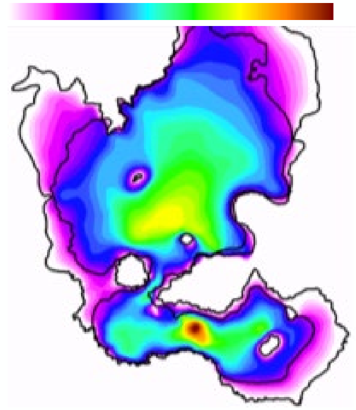

Ancient **lakes** (e.g. Texcoco) **were drained** and land was claimed **to build the Aztec capital** (XIV-XV cent.) and protect from flooding

Drainage continued over the centuries, plus **many wells were drilled to extract water** from the granular aquifer

The fine-grained (clay) aquitard compacts due to hydraulic heads declining due to pumping

Compaction rates correlate with aquitard thickness with a power function

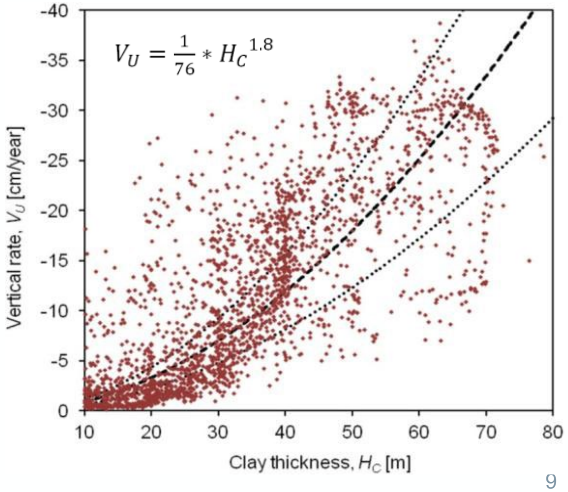

Hotspot #1 Mexico City: Angular distortions (β) and surface faulting

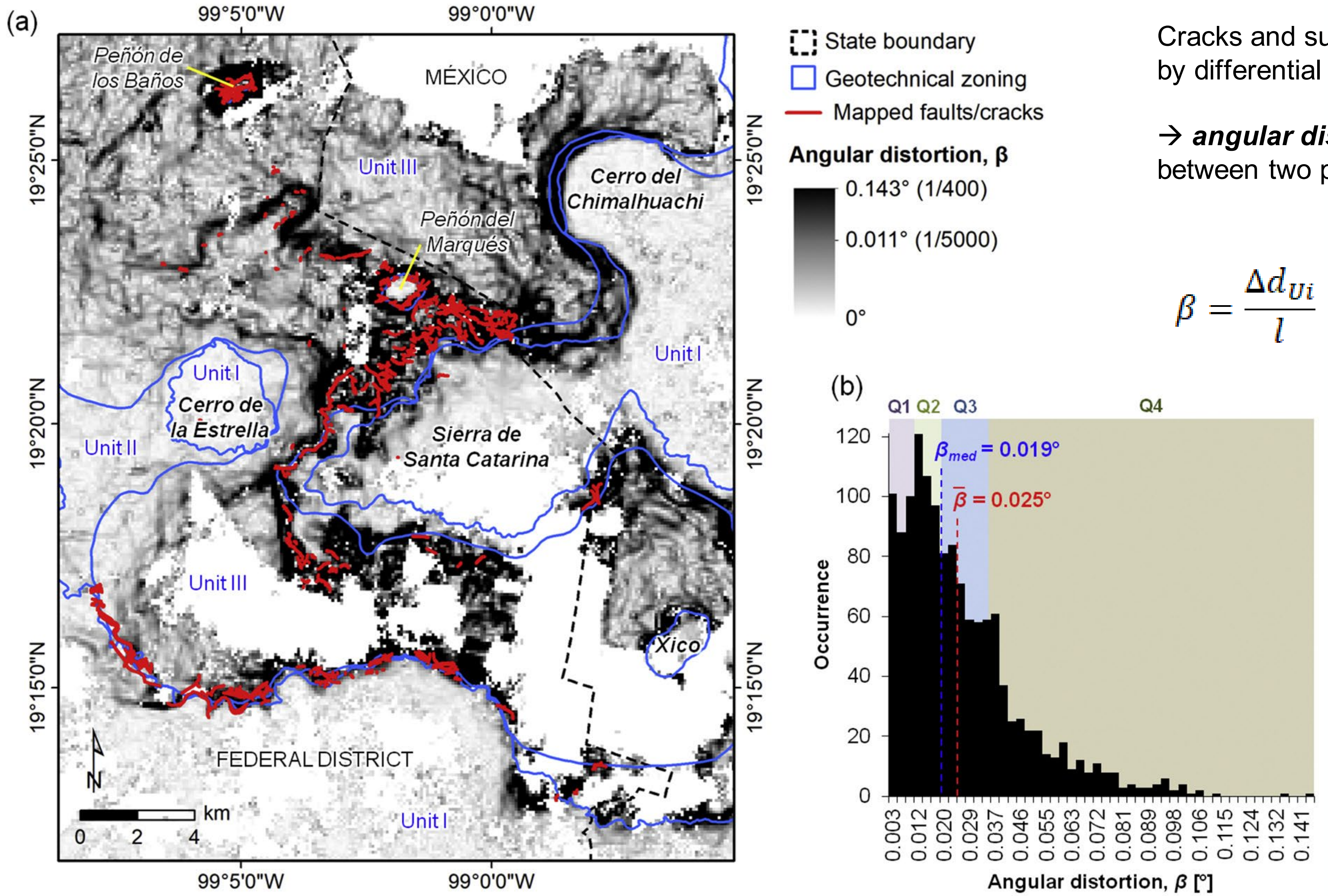

CIGNA & TAPETE 2021, doi:10.1016/j.rse.2020.112161

Cracks and surface faults mapped in the field concentrate in areas affected by differential settlement

→ ***angular distortion*** helps to quantify the amount of differential settlement between two points

$$\beta = \frac{\Delta d_{Ui}}{l}$$

Δd_{Ui} = differential settlement occurred between the two points
l = distance between the two points

High β → abrupt change in vertical deformation regime, hence higher potential for surface faulting to develop

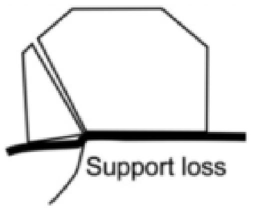

- β in 2017–2019 reaches 1/400, i.e. 0.14°
- Peaks at the transition unit (between lacustrine and volcanic units), e.g. at the foothills of volcano edifices

Hotspot #1 Mexico City: Risk assessment in urban AGEBs

***R**isk = **H**azard x **E**xposure x **V**ulnerability*

expected loss from a given natural hazard

Hazard: probability of occurrence of a potentially impacting phenomenon

Exposure: location, attributes and value of the assets that could be affected

Vulnerability: likelihood that the assets will be affected when exposed to the hazard

Angular distortions, β

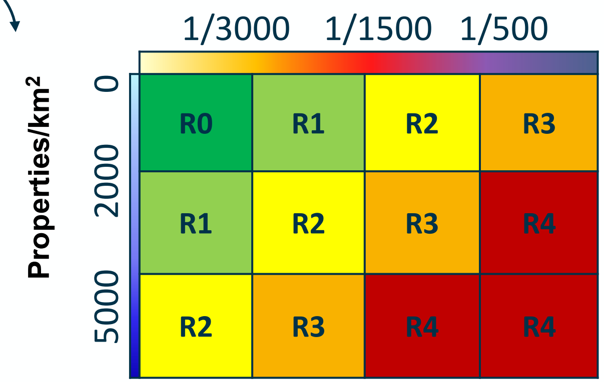

Output risk category

R0 – Very low
R1 – Low
R2 – Medium
R3 – High
R4 – Very high

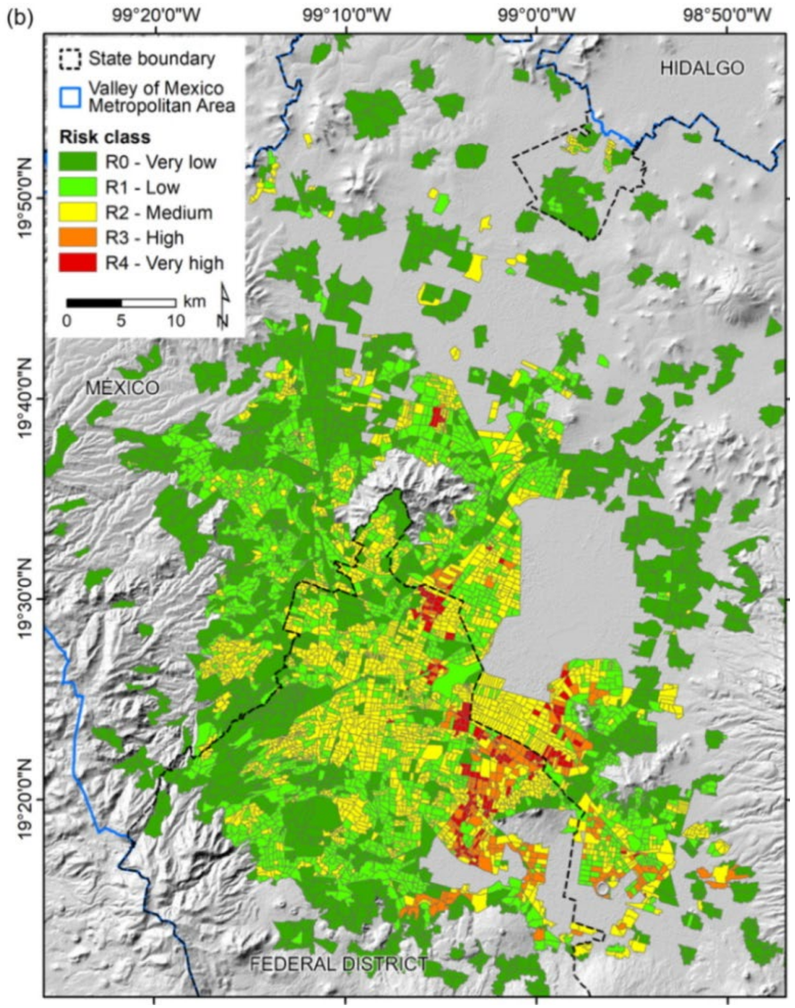

CIGNA & TAPETE 2021, doi:10.1016/j.rse.2020.112161

AGEB = 'basic geostatistical areas'

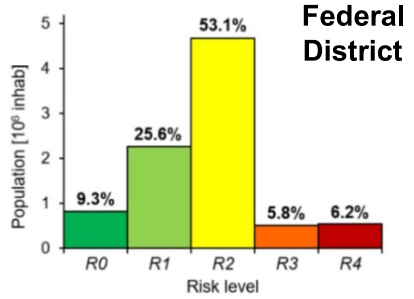

> 303,000 properties (out of ~2.7 millions) and
> 1 million inhab. (out of ~8.8 millions)
are in R3 or R4 areas

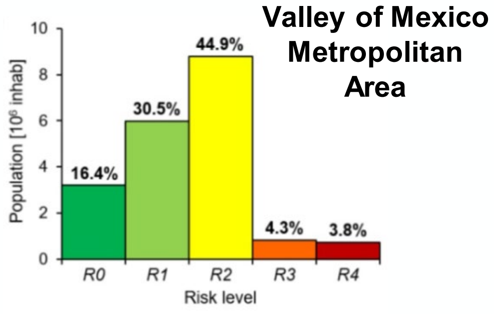

> 457,000 properties (out of ~6 millions) and
> 1.5 million inhab. (out of ~21.1 millions)
are in R3 or R4 areas

Hotspot #2 Morelia: Urban growth and land subsidence

The metropolitan area **expanded by +1.8 km²/year** in 1975–2020, with a boost in population growth (from ~400,000 inhab. in 1980 to >1 M in 2020) and water needs

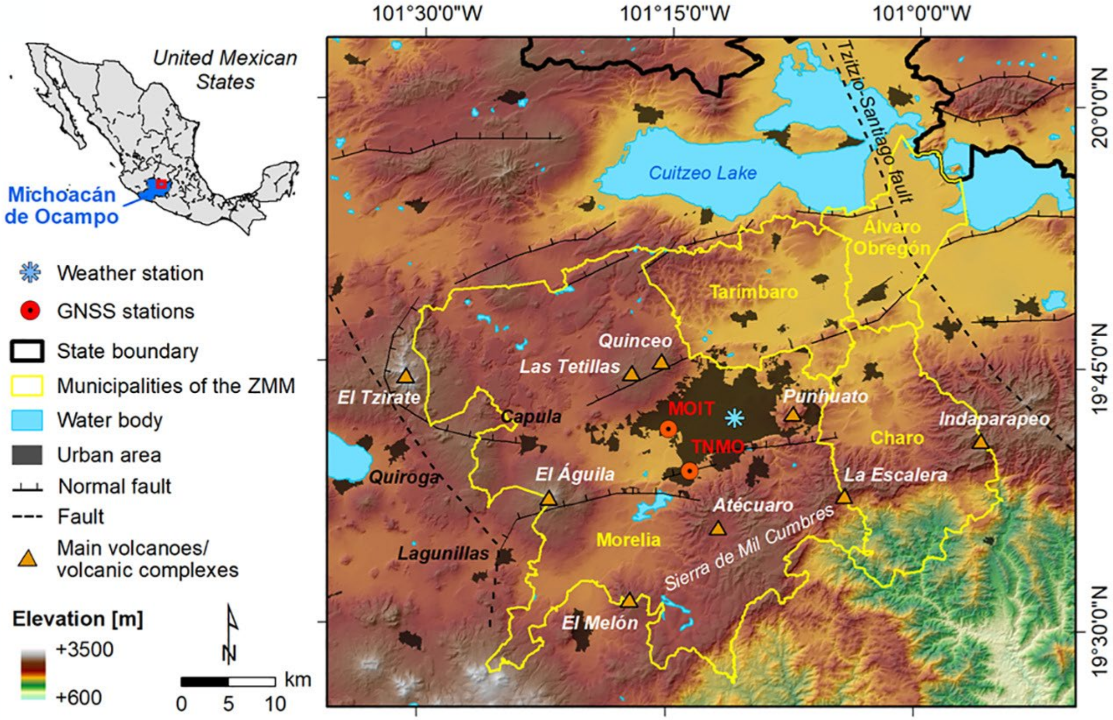

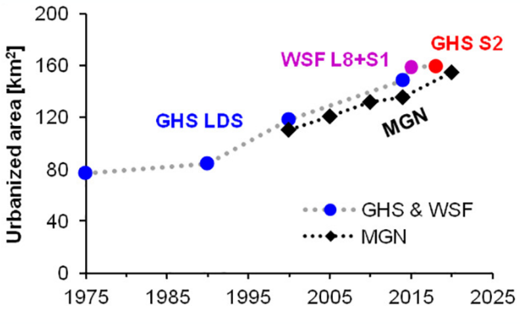

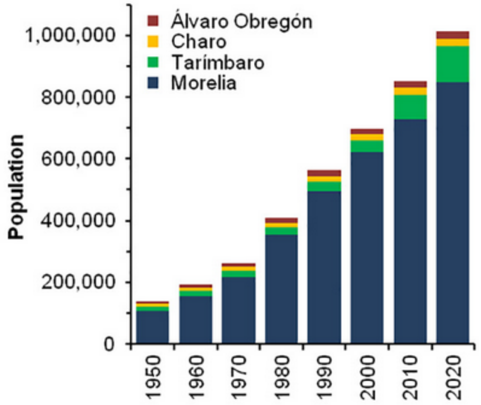

→ Differential sinking and **ground discontinuities are aligned with buried tectonic faults** and contrasting compressible sediment thickness

→ **Non-linearly deforming subsidence bowls** develop at extraction wells in both old and newly urbanized sectors

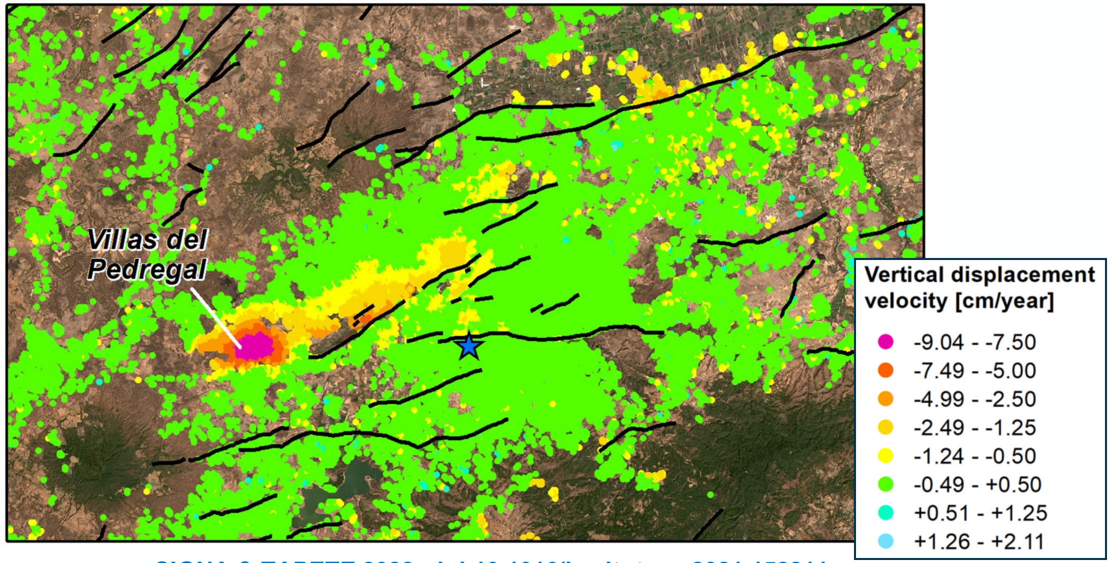

CIGNA & TAPETE 2022, doi:10.1016/j.scitotenv.2021.152211

Hotspot #2 Morelia: Newly developed housing neighborhood

New wells were drilled to address the boosted water demand of the new densely populated neighbourhood (**> 15,000 inhab./km²**)

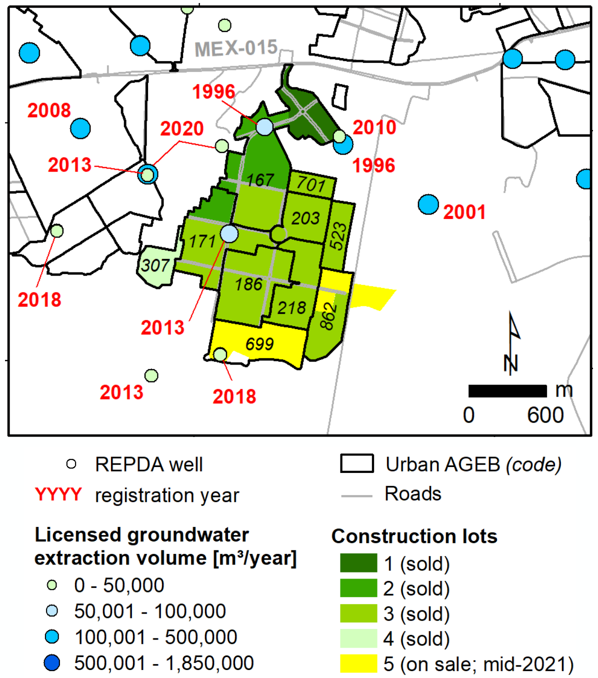

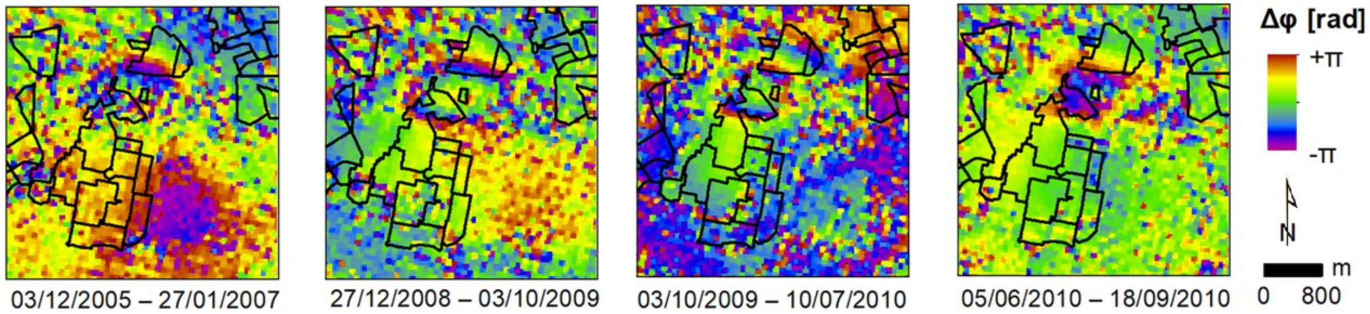

→ Time-lapse InSAR reveals **a rapidly subsiding bowl**, expanding and migrating following the sequence of new construction lots

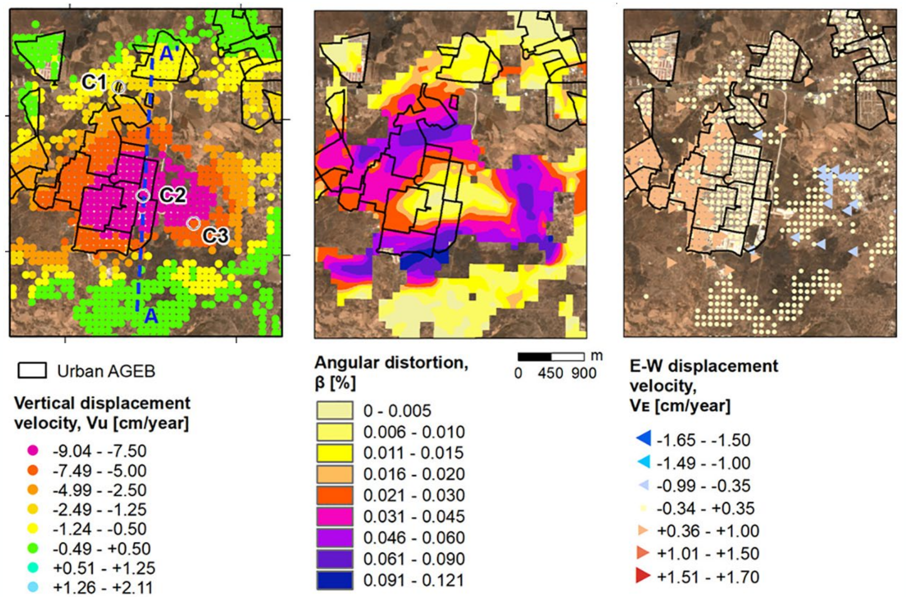

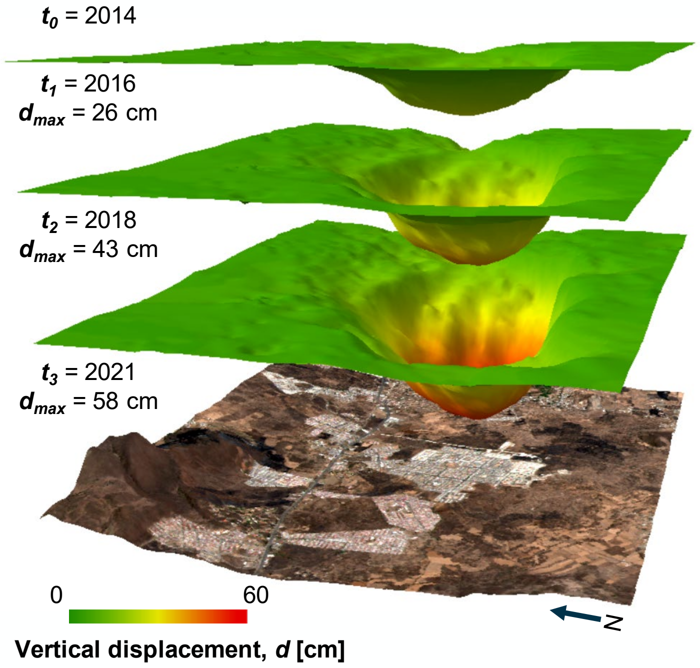

→ In 2014-2021, the bowl extends **4 km²**

→ With β reaching 0.12%, new buildings and roads are exposed to fracturing and surface faulting risk

CIGNA & TAPETE 2022, doi:10.1016/j.scitotenv.2021.152211

Hotspot #2 Morelia: Risk assessment in urban AGEBs & blocks

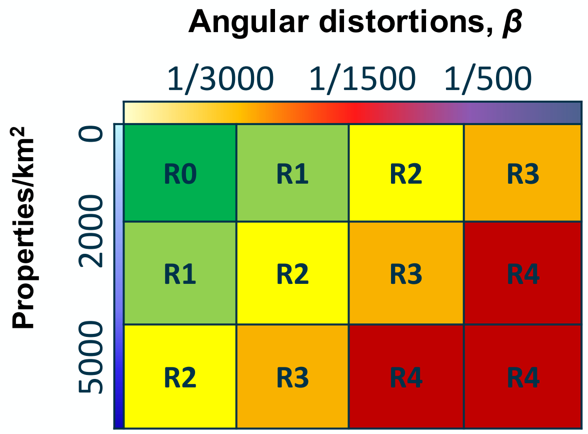

Output risk category

- R0 – Very low
- R1 – Low
- R2 – Medium
- R3 – High
- R4 – Very high

The analysis level can be **scaled down** to the **level of urban blocks**, to more precisely locate the elements at risk (properties) and fine-tune their risk assessment

<u>AGEB level</u>: 24,570 properties and > 48,700 inhab. are in R3 or R4 areas

<u>Block level</u>: > 8700 properties and 17,500 inhab. are in R3 or R4 areas

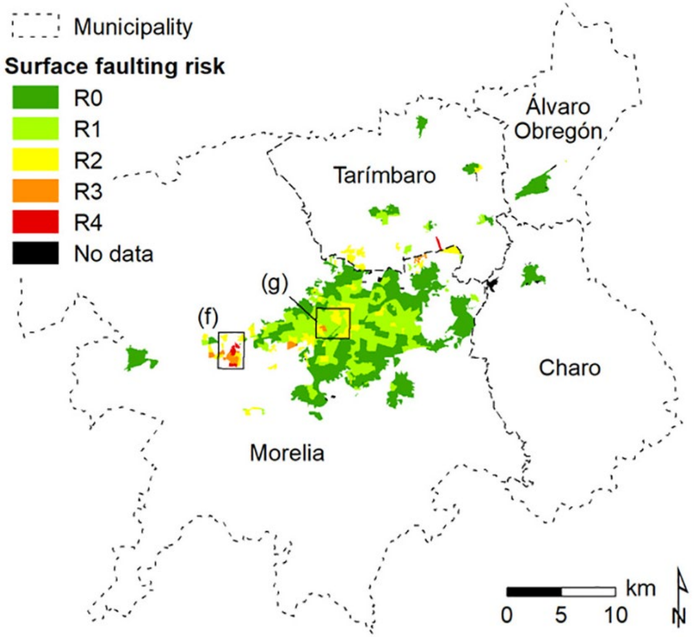

Urban AGEB level analysis

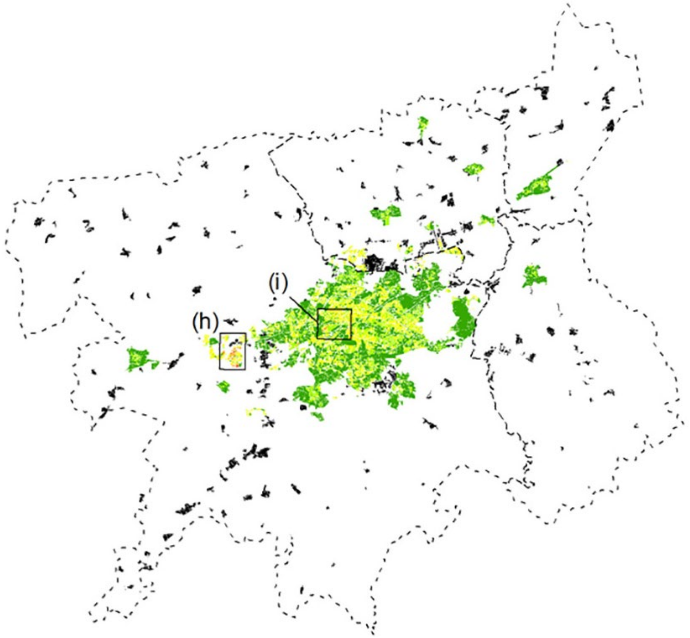

Urban block level analysis

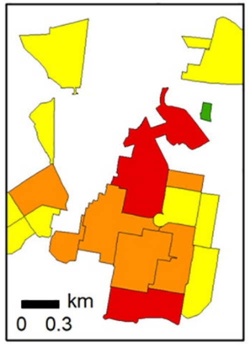

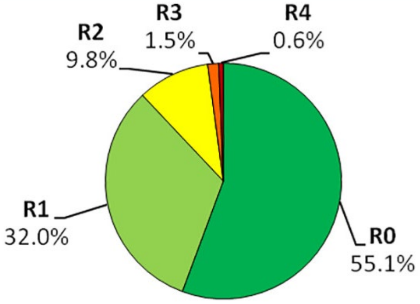

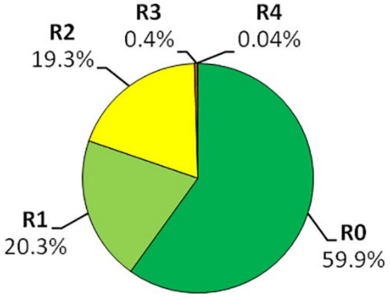

CIGNA & TAPETE 2022, doi:10.1016/j.scitotenv.2021.152211

Hotspot #3 Aguascalientes: Structurally-controlled subsidence

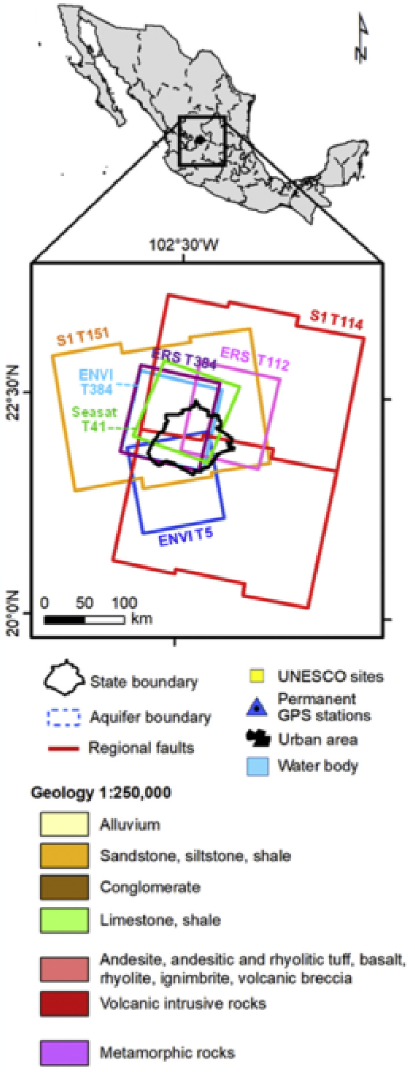

80 km-long valley bounded by N-S faults, running across the namesake state

Hundreds of wells drilled within the valley; the **aquifer is in deficit and overexploited**

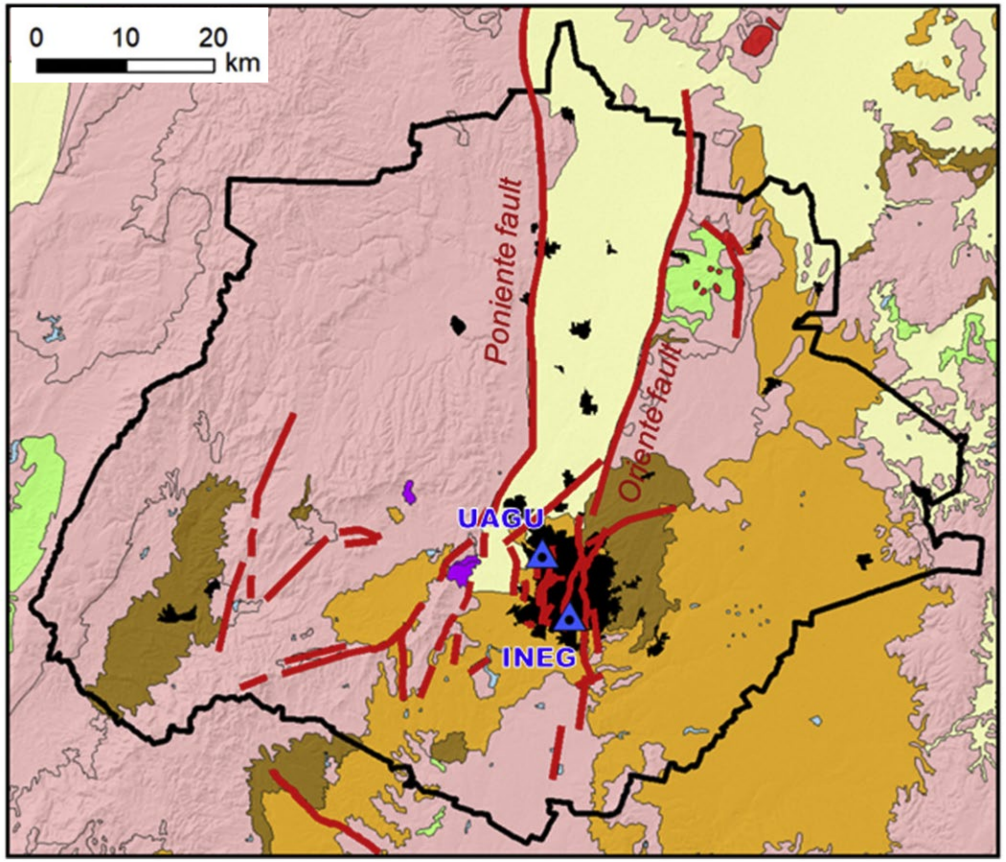

CIGNA & TAPETE 2021, doi:10.1016/j.rse.2020.112254

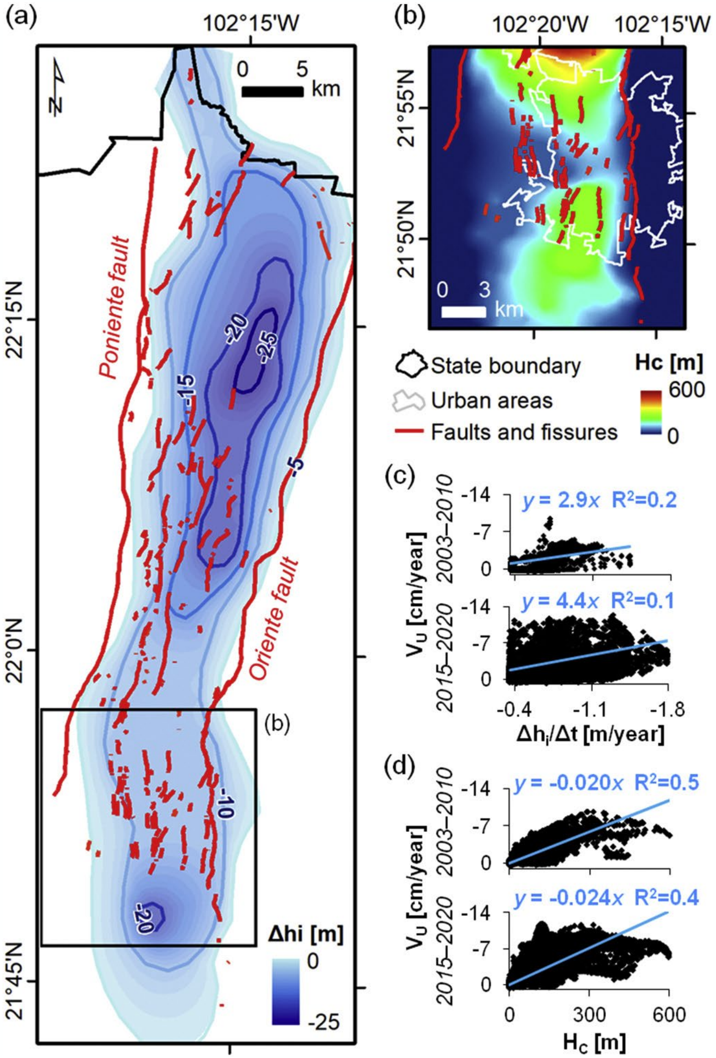

Hotspot #3 Aguascalientes: Vertical and E-W velocity field

Land deformation is dominated by vertical rates with subsidence bounded by the N-S faults, while **it also exhibits clear E-W components**, with deformation towards the center of the valley

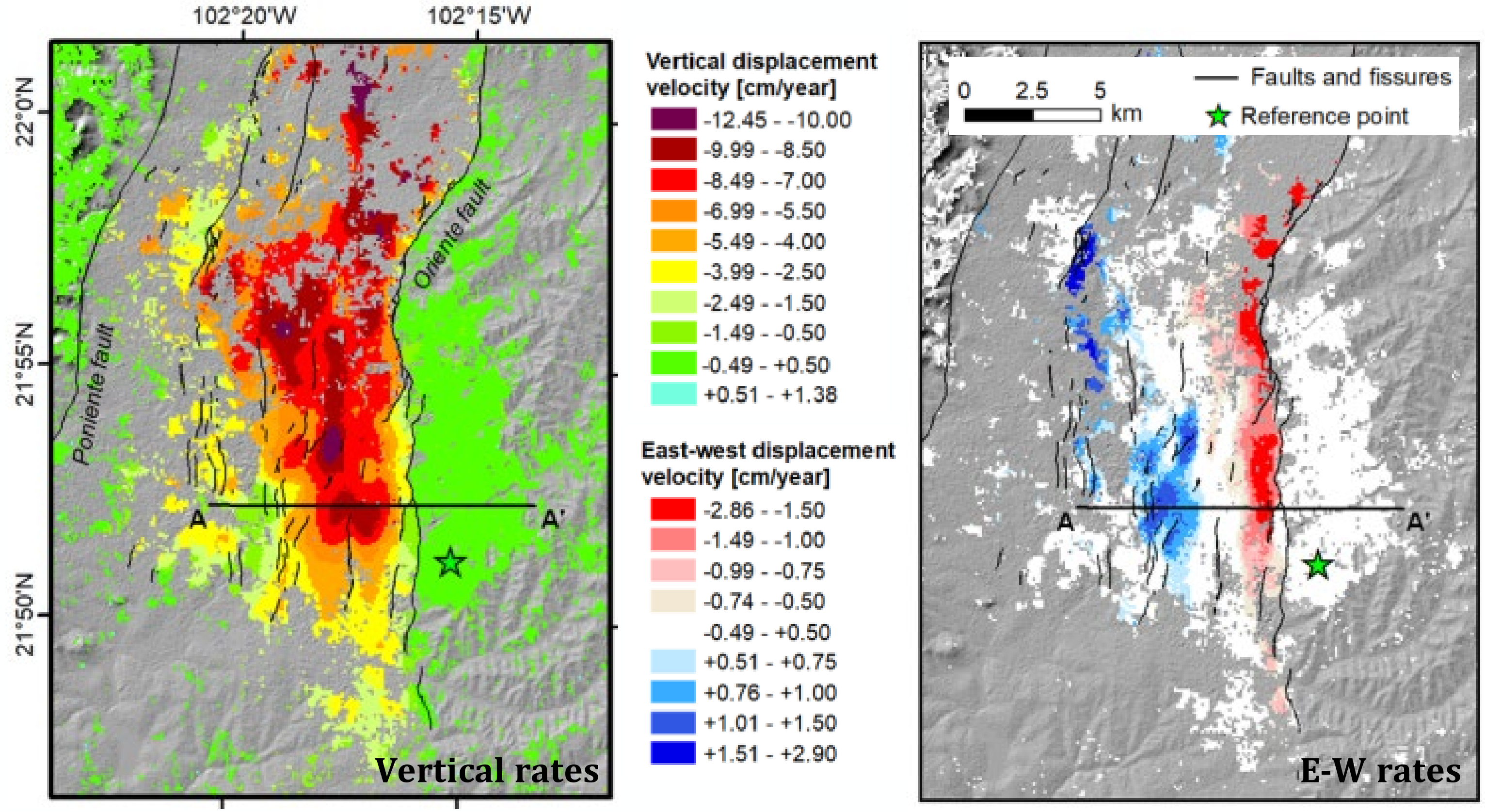

CIGNA & TAPETE 2021, doi:10.1016/j.rse.2020.112254

2015–2020 InSAR analysis → V_U up to –12.5 cm/year & V_E between ±2.9 cm/year

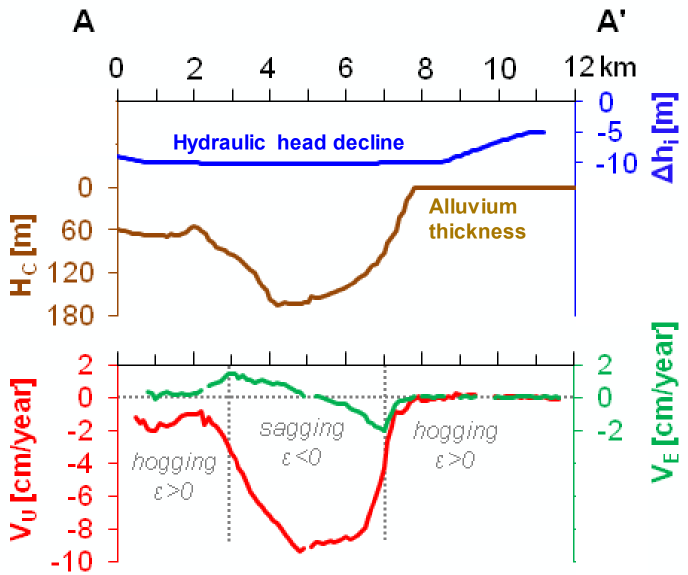

Significant **horizontal strain (ε)** is produced where the E-W rates change rapidly in space

$$\varepsilon = \frac{\Delta d_{Ei}}{l}$$

Δd_{Ei} = E-W displacement difference between the two points

l = distance between the two points

ε>0 → tensile strain (*hogging*)

ε<0 → compressive strain (*sagging*)

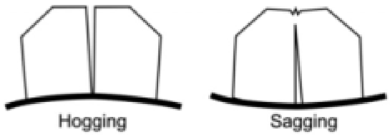

Hotspot #3 Aguascalientes: Risk assessment based on β and ε

Angular distortions, β

Properties/km² \ β	1/3000	1/1500	1/500	
0 – 2000	R0	R1	R2	R3
2000 – 5000	R1	R2	R3	R4
5000	R2	R3	R4	R4

Output risk category

- R0 – Very low
- R1 – Low
- R2 – Medium
- R3 – High
- R4 – Very high

If there is **significant horizontal strain (ε)**, the risk is increased by 1 level

if $|\varepsilon| \geq 0.03\%$ $\quad R_N \rightarrow R_{N+1}$

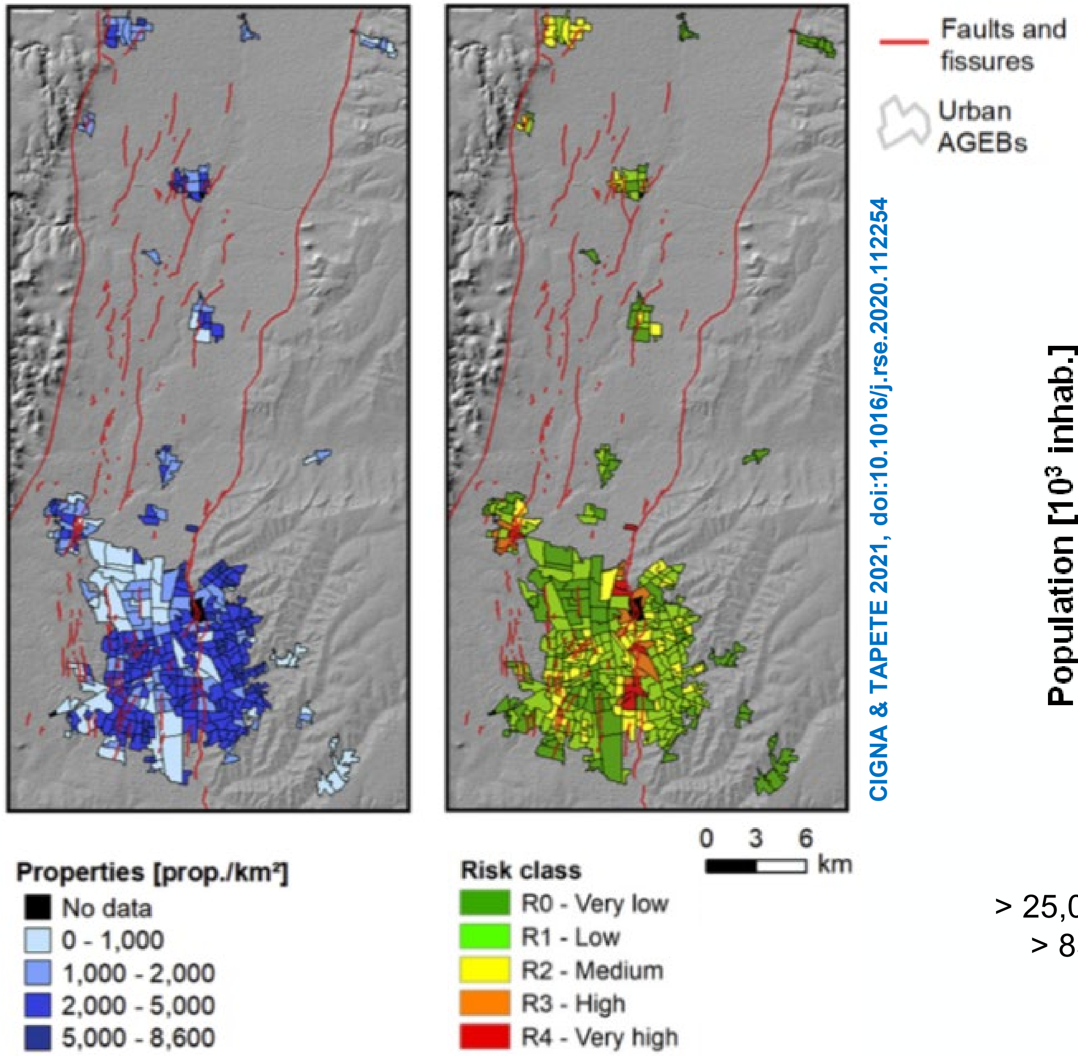

CIGNA & TAPETE 2021, doi:10.1016/j.rse.2020.112254

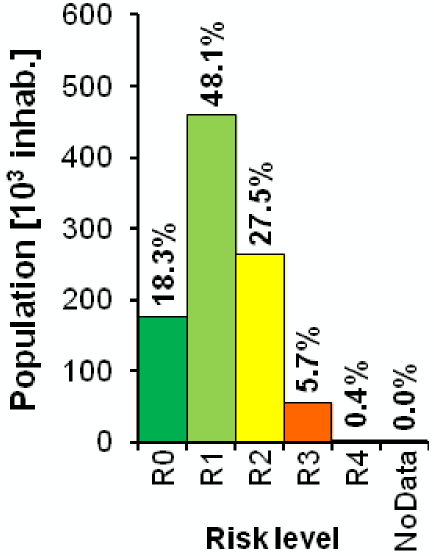

> 25,000 properties (out of 290,000) and
> 85,000 inhab. (out of 1.3 millions)
are in R3 or R4 areas

Key conclusions & messages for the Round Table

- The quasi-continental InSAR survey and the derived risk maps at the **subsidence hotspots** prove valuable to constrain the land deformation process, derive semi-theoretical relationships between groundwater balance parameters and land subsidence, locate and quantify urban properties at risk – **Sentinel-1 observation continuity must be ensured to update assessment over time**
- Such quasi-continental surveys and dense local-scale assessments are more feasible if InSAR processing is facilitated – **crucial roles of InSAR processing platforms that should be kept easily accessible to users**
- InSAR-derived products are useful knowledge-base for policy makers and regulators to optimize groundwater resource management, accommodate existing and future water demands, and try not to further exacerbate aquifer-system storage loss – **Sentinel-1 observation continuity enables the update of downstream application products**
- Risk analysis at urban blocks level allows for a refined risk assessment scale capability (vs. the urban AGEB level) – next steps: VHR SAR data
- More data on elements at risk (building type, height, maintenance status) would enable further improvement of the risk assessment workflow

 # Full papers #

CIGNA F., TAPETE D. 2021. Present-day **land subsidence** rates, surface faulting hazard and risk in **Mexico City** with 2014-2020 Sentinel-1 IW InSAR. *Remote Sensing of Environment*, 253, doi:10.1016/j.rse.2020.112161

CIGNA F., TAPETE D. 2021. Satellite InSAR survey of **structurally-controlled land subsidence** due to groundwater exploitation in the **Aguascalientes Valley**, Mexico. *Remote Sensing of Environment*, 254, doi:10.1016/j.rse.2020.112254

CIGNA F., ESQUIVEL RAMÍREZ R., TAPETE D. 2021. **Accuracy of Sentinel-1 PSI and SBAS InSAR** displacement velocities against GNSS and geodetic leveling monitoring data. *Remote Sensing*, *13*, 4800, doi:10.3390/rs13234800

CIGNA F., TAPETE D. 2022. **Urban growth** and land subsidence: Multi-decadal investigation using human settlement data and satellite InSAR in **Morelia**, Mexico. *Science of the Total Environment*, 811, doi:10.1016/j.scitotenv.2021.152211

CIGNA F., TAPETE D. 2022. Land subsidence and aquifer-system storage loss in Central Mexico: A **quasi-continental investigation** with Sentinel-1 InSAR. *Geophysical Research Letters*, 49(15), e2022GL098923, https://doi.org/10.1029/2022GL098923